Co-channel Secondary Deployment over DTV Bands using Reconfigurable Radios

Anshul Thakur, Swades De, and Gabriel-Miro Muntean

***Abstract*—This paper investigates the possibility of co-channel secondary transmission over the operational digital terrestrial video (DTV) broadcast bands within the interference limits of the DTV receivers. Aided by emulated DTV transmission experiments, secondary transmission-caused interference to the DTV receiver is analyzed in the context of a DTV network. Using this understanding of interference behavior, a new transmission scheme for the secondary network nodes is proposed. The scheme selects the best communication parameters in terms of transmit power, spectral overlap, temporal occupancy, symbol duration, and modulation scheme to achieve a desired quality of service target within the interference limits of the DTV receivers. This is achieved without having information about the presence of DTV receivers. The feasibility as well as limits of the proposed secondary deployment scheme are then analyzed. This study is expected to serve as a valuable planning tool in deploying cognitive secondary networks over DTV transmission bands.**

***Index Terms*—Co-channel interference, DTV band transmission, cognitive radio, optimal parameter selection**

I. Introduction

With the advent of fifth generation (5G) networks and Internet of Things (IoT) communications, the demand for increased wireless coverage and higher data rates have increased manyfold. In order to address the challenges associated with this increased demand on wireless spectrum, two major strategies have emerged. One approach is to allocate more spectrum by making previously unallocated higher frequency bands available. The other approach is to improve the spectrum utilization in the already-allocated lower frequency bands.

Allocation of more spectrum at higher frequencies typically requires dense deployment due to high path loss. Dense deployment of infrastructure by network providers offers greater data rate and better spatial reuse of frequencies and capacity. At the same time, poor economies of scale hinder widespread infrastructure deployment, particularly in sparsely-populated rural areas. Consequently, such rural areas lack access to data networks offering good capacity and coverage.

This work has been supported in parts by the ITRA Media Lab Asia project, Government of India, under Grant no. ITRA/15(63)/Mobile/MBSSCRN/01, and by the Department of Telecommunications, Government of India, under the Grant no. 4-23/5G test bed/2017-NT for building end to end 5G testbed. The support of Science Foundation Ireland (SFI) Research Centres Programme grants SFI/12/RC/2289_P2 (Insight) and 16/SP/3804 (ENABLE) is also gratefully acknowledged.

A. Thakur is with Center for Development of Telematics, New Delhi, and the Department of Electrical Eng., IIT Delhi, New Delhi, India (e-mail: anshul.thakur@ee.iitd.ac.in). S. De is with the Department of Electrical Eng., IIT Delhi, New Delhi, India (e-mail: swadesd@ee.iitd.ac.in). G.-M. Muntean is with the Performance Engineering Laboratory, School of Electronic Eng., Dublin City University, Ireland (e-mail: gabriel.muntean@dcu.ie).

A preliminary version of the work was presented at the IEEE International Conference on Communications, Shanghai, China, May 2019 [1].

On the other hand, improving spectrum utilization in the allocated bands in lower frequencies calls for novel ways of spectrum access and reuse [2]. The lower end of the UHF band is a particularly attractive band for such research as it has excellent propagation characteristics. So far, this part of the spectrum has primarily been used by television (TV) and radio broadcasting services. Regulatory bodies across the world are rapidly realizing the need to open up this part of the spectrum for other communication services. As a result, many regulatory agencies have been in the process of allowing opportunistic use of parts of these TV bands to increase spectrum utilization.

In the upcoming digital TV (DTV) broadcast services, new paradigms of coexistence among digital broadcast and other digital communication services are being explored. Standards like IEEE 802.11af, IEEE 802.22 Wireless Regional Area Network (WRAN) and Long-Term Evolution in Unlicensed Spectrum (LTE-U) have been ratified to claim the TV White Spaces (TVWS) that are found to exist in the TV bands. In all these technologies the secondary nodes rely on a geolocation database that maintains the TVWS frequency occupancy across different geographical regions to find an operating frequency. Further, in conventional practice, if there is an ongoing TV broadcast transmission, there exists a coverage radius in which its transmission is held sacrosanct wherein no one else is allowed to transmit in the same band.

However, it is also this protected region where the received DTV signal levels are expected to be well above the desired minimum signal interference and noise (SINR) threshold. The availability of excess signal strength may be opportunistically exploited by the secondary communication network for its own benefit, without degrading the DTV reception quality.

In cellular communications, the concept of spectrum reuse by co-channel deployment is already a part of the LTE standard [3], where small-cells are deployed within a macro-cell using a set of frequencies that may interfere with the macro-cell transmissions. Limited spectrum pooling and spectrum sharing is also practiced to increase spectrum efficiency [4].

Aiming at efficient usage of TV spectrum to fulfill steep bandwidth demand for rural broadband access, in this work co-channel secondary transmission is explored. A signal-level description of the two systems is employed to analyze the interference on DTV receiver. Secondary transmission parameters can be varied dynamically, enabling to stay below a permissible interference level for DTV reception.

A. Key contributions

The major contributions of this paper are as follows:

1) A general framework for analyzing co-channel interference in orthogonal frequency division multiplexing

(OFDM) systems is presented. The impact of secondary co-channel transmission on DTV receiver is validated through extensive experimental work and simulations. It is shown that the aggregate impact of secondary network is largely determined by the extent of spectral and temporal overlaps between DTV signal and secondary signal.
2) Coexistence between DTV broadcast and secondary communications is demonstrated by secondary network's flexibility over multiple dimensions, namely, power control, link scheduling, and spectral occupancy over DTV bands. The analytical observations are corroborated via experimental studies, which also compare the performance of LTE-like transmissions with 802.11af-like transmissions.
3) A novel QoS-aware low interference secondary parameter selection based transmission protocol, called LISP transmission, is proposed, which works without the knowledge of channel states in DTV transmission and location of DTV receivers. LISP transmission ensures that the interference experienced by a potential DTV receiver in the vicinity does not exceed a certain threshold.
4) Additionally, an exhaustive parameter search (EPS) algorithm is proposed to find working parameters of the secondary nodes, and performance limits of LISP transmission for co-channel secondary link are studied.

This study shows that long-range mid-haul connectivity as secondary communication over TV bands for rural broadband access is more feasible in less populated areas. In such deployments, the LISP transmission scheme will not necessarily need to find an empty TV band through a database query. Further, the analytical expressions developed in this study can be used for a wider range of applications where the impact of interference between OFDM systems needs to be assessed.

B. Paper organization

Next section contains a brief literature survey. Section III outlines the system model and assumptions. In Section IV, a signal level model of DTV and secondary transmission is used to derive closed-form expressions of interference to a DTV receiver. By considering non-availability of channel state knowledge in DTV transmission and DTV receivers' location information, in Section V, LISP transmission scheme and the EPS algorithm are proposed to compute the operational parameters of the secondary link that maximize its data rate. Experimental and simulation based performance evaluation are presented in Section VI. The paper is concluded in Section VII.

II. Related Work

Coexistent co-channel communication improves spectral efficiency, however interference among contending technologies could be sometimes unacceptable. In OFDM, interference can lead to severe degradation of quality due to loss of orthogonality between subcarriers. Effects of narrow-band interferers on OFDM reception and the methods of mitigating these effects were studied in [5], [6] by modeling the post-DFT (discrete Fourier transform) effects of interference on each subcarrier symbol detection. However, service quality degradation was not analyzed in these works. The effects of narrow-band interference on the primary OFDM signal using power spectral density (PSD) of the associated signals were investigated in [7], [8]. Taking the frequency spectrum of an OFDM subcarrier as a $sinc$ function, these studies estimated the effect of one or a few narrow-band interference sources on the OFDM signal using relative interference power as a metric.

Studies on co-channel interference among OFDM-based systems have mostly catered to homogeneous settings like cellular networks where the interferer is a nearby cell operating with the same parameters. The effects of carrier frequency offset on OFDM performance were studied in [9]–[11]. Other co-channel interference due to self-generated artifacts have mostly been mapped on to changes in carrier frequency offset and were studied from that perspective. The study in [12] showed that the above approach and the PSD based approach overestimate the interference levels as they do not consider misalignment between the coexisting parties. Also, such analyses do not extend well to heterogeneous OFDM systems where significant differences between the signal structures exist which cannot be simplified to just carrier offsets.

Methods to improve spectral efficiency can be broadly classified into three: underlay, overlay, and interweave schemes. Overlay techniques require some degree of cooperation among the participating networks, whereas interweave techniques work on the principle that spectrum occupancy by the primary is not constant. Underlay schemes work towards keeping the interference to the primary receivers below a specified level.

In the DTV bands, regulatory bodies have currently adopted an open-loop regulatory framework of mutually exclusive access to the TV spectrum that avoids the issue of co-channel interference. It is akin to interweave method where a secondary network trying to transmit in the TV bands must first query a geolocation database, which grants access to a channel if no TV broadcaster is using it at that time and location [13]. Parts of this method have been demonstrated through several experimental case studies in the growth markets, such as Latin America, India [14], Africa [15], and Southeast Asia with major industry partners like Microsoft Research. In the Indian context, an LTE based two-stage mid-haul TVWS deployment between a few POP nodes and the rural outreaches was studied in [16], where TVWS carries data to homesteads and is further distributed to the household users over WiFi. The use of geolocation database for message delivery in vehicular networks is studied in [17]. Spectrum sharing among the operators was studied in [18] with a graph-theoretic approach for Fairness Constrained Channel Allocation employing Carrier Aggregation and Listen Before Talk features of LTE-A. It was noted in [19] that the above approach would increase infrastructure costs when covering sparsely-populated rural areas. Accordingly, the use of collaborative beamforming by forming clusters in the rural area was proposed. However, these approaches work in TVWS access mode.

On the other hand, several researchers have studied the possibility of co-channel operation between a broadcast network and another OFDM-based secondary communication network, namely LTE [20] and IEEE 802.22 WRAN [21]. Coexistence of TV broadcast technologies like Digital Video Broadcast-Terrestrial (DVB-T) and its second generation DVB-T2 with

IEEE 802.22 and other OFDM based systems was studied in laboratory environments [22], [23]. These works were based on controlled experimental testbeds or numerical simulations, where the interference was studied to determine the acceptable level of interference in the form of Carrier-to-Interference (C/I) ratio, for various transmission parameters of the DVB system. Some operating configurations in which an interferer may impact the DVB reception, or in some converse cases where DVB acts as an interferer, were reported in [21]–[23]. C/I protection ratios required for LTE-A femtocell operation indoors while having varying degrees of channel overlap with the primary DTV broadcast were evaluated in [24]. These studies indicated that the impact of interference is small for small overlaps between frequency bands of the DVB and secondary networks. The operating configurations in which an LTE system may be deployed depending on the amount of spectral overlap were experimentally evaluated in [25]. A signal-level description of mutual interference between DVB-T2 and LTE was studied in [26], where the authors optimized spectral overlap to maximize net channel capacity while considering some degree of interference cancellation on all receivers. However, all of these studies focused on coexistence of the existing technologies deployed as-is, without accounting for the key differences in signal structures, framing, and link-scheduling of the two heterogeneous technologies. These differences were explored in [1] by considering a discrete time approach to analyzing the co-channel interference. However, it made simplified assumptions, such as a large disparity between the number of subcarriers in the DTV signal and in the secondary signal. The discrete time approach and the model assumptions restricted the applicability of the approach to select cases. Neither did these studies consider the effect of such co-channel operation on the secondary system from a deployment point of view, nor do these suggest any viable deployment scheme.

In a conventional underlay scheme, complete or partial channel state information between the primary transmitter and receiver path is assumed available [27] by either decoding the feedback messages or overhearing the conversation and inferring the information from it to exercise interference control. Owing to the fixed transmission parameters and unidirectional nature of DTV broadcast, detection of DTV receivers actively tuned to a channel in an area is highly challenging. Detection of a DTV receiver via its local oscillator's leakage power [28] requires the secondary nodes to be placed very near to the DTV receiver which may not always be feasible. Methods like attaching additional devices to the DTV receivers, such as smart remotes [29] and Nielson TV meters [30] for collecting TV usage statistics, deviate significantly from the underlay approach.

In such cases, the secondary system can only take a conservative view and work with some statistics on DTV receiver locations. One way to estimate signal conditions at the potential TV receiver locations is to rely on the channel gain cartography [31]. Trilateration is used to compute the relative locations of the DTV transmitter and secondary receiver through Received Signal Strength Indicator (RSSI) measurements. The secondary transmitter uses this information to find operational parameters which ensure that the interference experienced by a DTV receiver does not exceed a threshold. Co-channel interference needs to be estimated to enable this computation.

It is seen that the existing case studies which deploy secondary networks use the geolocation database for gaining exclusive access to a channel which circumvents the issue of interference. This ignores the possibility that there might be no active consumers of the broadcast in the desired coverage area of the secondary system. Studies analyzing co-channel interference in homogeneous OFDM systems do not extend well into the present case of heterogeneous OFDM system involving a DTV broadcast and a secondary communication system. Empirical studies have established C/I ratios that must be maintained at a DTV receiver to avoid experiencing poor reception quality. However, these studies have not exploited various differences between the broadcast technology and the competing secondary technology, such as the differences in coverage areas, power margins, and symbol durations. Conventional underlay schemes also cannot be applied due to lack of any form of feedback from the DTV receivers.

To this end, this work first presents an analysis of co-channel interference at the DTV receiver which highlights how the differences between the broadcast technology and the secondary technology can be used to reduce interference. LISP transmission scheme is then proposed for the secondary nodes to choose their transmission parameters conservatively, thus sustaining a secondary network communication without disrupting the viewing experience of any potential DTV receiver. The system model introduced in the next section will be used to estimate this co-channel interference at a DTV receiver.

III. System Model

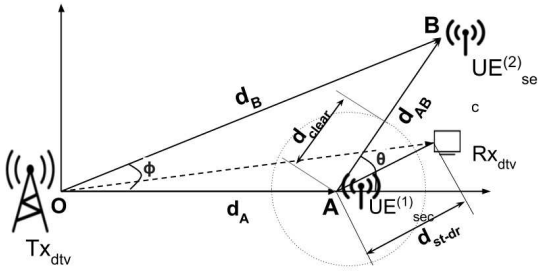

Fig. 1. Schematic view of secondary communication in DTV coverage range.

Let us consider the system setting illustrated in Fig. 1, where a secondary transmitter $\text{UE}_{\text{sec}}^{(1)}$ and a receiver $\text{UE}_{\text{sec}}^{(2)}$ are positioned in the coverage region of a DTV transmitter Tx_{dtv} at distances d_A and d_B from Tx_{dtv}, respectively. Transmission power of Tx_{dtv} is $P_{tx}^{(D)}$, whereas $\text{UE}_{\text{sec}}^{(1)}$ transmission power is $P_{tx}^{(S)}$. Hence, secondary receiver $\text{UE}_{\text{sec}}^{(2)}$ located at a distance d_{AB} from the secondary transmitter receives average powers of $P_{rx}^{(D)}$ and $P_{rx}^{(S)}$, respectively, due to the DTV broadcast and secondary transmission. For simplicity, only the effect of communication from $\text{UE}_{\text{sec}}^{(1)}$ to the $\text{UE}_{\text{sec}}^{(2)}$ which is at a greater distance from the DTV transmitter than $\text{UE}_{\text{sec}}^{(1)}$ ($d_B \geq d_A$) is considered. The analysis remains valid in the reverse direction from $\text{UE}_{\text{sec}}^{(2)}$ to $\text{UE}_{\text{sec}}^{(1)}$, though the maximum allowed transmit power is reduced due to increased distance from Tx_{dtv}. The

DTV receivers are assumed to experience a good SNR in the absence of interference. Consequently, the effects of multipath fading as well as shadowing are considered to be mitigated. A path-loss exponent of $\eta^{(D)}$ is considered for link-budget computations.

An out-of-band signaling is considered among secondary nodes for exchanging control information, such as received RSSI due to the secondary peer and DTV transmitter and operational parameters. The propagation environment is assumed to exhibit log-normal shadowing. A combined shadowing and path loss model is assumed for path-loss computations for the secondary network with a path-loss exponent of $\eta^{(S)}$. The secondary nodes can choose from a fixed set $\mathbb{R}^{(S)}$ of modulation and coding schemes (MCS). Each MCS requires a minimum SNR for proper operation. The secondary nodes are located within DTV coverage area and the $\text{UE}_{\text{sec}}^{(1)}$ to $\text{UE}_{\text{sec}}^{(2)}$ distance is such that a minimum SNR for at least one MCS scheme is achievable. The secondary devices are assumed capable of receiving DTV transmission and use it for interference cancellation at their end. For interference study, a DTV receiver Rx_{dtv} is assumed present in between the two communicating secondary nodes, at a distance d_{st-dr} from the secondary transmitter. The interference experienced by this DTV receiver is the subject of Section IV.

The DTV broadcast network as well as the secondary network use OFDM technology but with different physical characteristics and parameters, such as different subcarrier spacing and frame durations. DTV employs $N^{(D)}$ active subcarriers while the secondary system employs $N^{(S)}$ active subcarriers. $N^{(S)}$ is variable subject to a maximum value set by the physical transmission scheme in use. Similarly, $T^{(x)}$, $T_u^{(x)}$, and $T_g^{(x)}$ are the total symbol durations, useful symbol durations, and guard periods for the transmission network $x \in \{D, S\}$, where D and S respectively represent digital broadcast network and secondary OFDM network. Since DTV symbol duration is quite large to account for large delay spreads arising out of its large coverage area as compared to the secondary systems, the condition $T_u^{(D)} \gg T_u^{(S)}$ is assumed. A glossary of all symbols used in this paper are listed in Table I. In the next section, the interference due to co-channel secondary transmissions on Rx_{dtv} is analyzed.

TABLE I
GLOSSARY OF SYMBOLS USED

Notation	Description
$s^{(D)}(t)$	Transmitted DTV signal
$r^{(D)}(t)$	Received DTV signal at the DTV receiver
$r^{(S)}(t)$	Received secondary signal at the DTV receiver
$T^{(D)}$	Total symbol duration of DTV signal
$T^{(S)}$	Total symbol duration of secondary signal
$T_u^{(D)}$	Useful symbol duration of DTV signal
$T_u^{(S)}$	Useful symbol duration of secondary signal
$T_g^{(D)}$	Guard interval in DTV signal
$T_g^{(S)}$	Guard interval in secondary signal
L'	Number of multipath components for DTV signal
L	Number of multipath components for secondary signal
l'	Index of DTV signal's symbol block
l	Index of secondary signal's symbol block
$\tau_{n'}$	Signal delay in the n'th multipath of DTV signal
τ_n	Signal delay in the nth multipath of secondary signal
t_{off}	Random delay between the arrival of a DTV symbol and its first interfering secondary signal ($l' = 0$)
$N^{(D)}$	Total subcarriers in DTV signal
$N^{(S)}$	Active subcarriers in secondary signal
$N_{\max}^{(S)}$	Maximum subcarriers in secondary signal
ξ'	Number of symbol slots occupied by secondary in $T^{(D)}$
$\xi'_{\max}$	Maximum number of secondary symbol slots in $T^{(D)}$
$P_{tx}^{(D)}$	Power transmitted by the DTV transmitter
$P_{tx}^{(S)}$	Power transmitted by the secondary transmitter
$P_{rx}^{(D)}$	DTV signal power received by the DTV receiver
$P_{rx}^{(S)}$	Secondary signal power received by the DTV receiver
$\Phi_{p'}$	OFDM basis function for the p'th DTV subcarrier
$\eta^{(D)}$	Path loss exponent for DTV signal
$\eta^{(S)}$	Path loss exponent for secondary signal
$I_{p'}$	Interference on the p'th DTV subcarrier due to secondary co-channel transmission
γ_{dtv}	Average SINR experienced at the DTV receiver
γ_{th}	Average SINR threshold at the DTV receiver
$\mathbb{R}^{(S)}$	Set of MCS supported by the secondary system
$R^{(S)}$	MCS from $\mathbb{R}^{(S)}$ by the secondary transmitter
SNR^R	SNR achieved for the selected MCS $R^{(S)}$
$SNR_{\min}^R$	Minimum SNR required for the selected MCS $R^{(S)}$
d_A	DTV transmitter to secondary transmitter distance
d_B	DTV transmitter to secondary receiver distance
d_{AB}	Secondary transmitter to secondary receiver distance
d_{st-dr}	Secondary transmitter to nearest DTV receiver distance
d_{clear}	Minimum separation between secondary transmitter and DTV receiver to avoid excess interference

IV. DTV Reception Interference Analysis

Let $s^{(D)}(t)$ be the signal transmitted by the DTV transmitter Tx_{dtv}. $s^{(D)}(t)$ can be expressed as:

$$s^{(D)}(t) = \frac{1}{\sqrt{T_u^{(D)}}} \sum_{l' \in \mathbb{Z}} \sum_{k'=0}^{N^{(D)}-1} X_{k'}^{(D)}[l'] e^{j2\pi \frac{k' t}{T_u^{(D)}}} \prod \left(\frac{t - l' T^{(D)} + T_g^{(D)}}{T^{(D)}} \right) \tag{1}$$

$N^{(D)}$ is the number of active subcarriers in the DTV network, $X_{k'}^{(D)}$ is the data symbol transmitted in the l'th block on the k'th subcarrier. $T_u^{(D)}$ and $T_g^{(D)}$ are respectively the useful symbol period and guard interval, with $T^{(D)} = T_u^{(D)} + T_g^{(D)}$.

At the DTV receiver, the signal $r^{(D)}(t)$ is expressed as:

$$r^{(D)}(t) = \frac{1}{\sqrt{T_u^{(D)}}} \sum_{l' \in \mathbb{Z}} \sum_{n'=1}^{L'} \sum_{k'=0}^{N^{(D)}-1} h_{n'}^{(D)} X_{k'}^{(D)}[l'] e^{j2\pi \frac{k'(t-\tau_{n'})}{T_u^{(D)}}} \cdot \times \prod \left(\frac{t - l' T^{(D)} + T_g^{(D)} - \tau_{n'}}{T^{(D)}} \right) \tag{2}$$

where L' is the number of multipath components of the DTV signal, $\tau_{n'}$ and $h_{n'}^{(D)}$ are respectively the delay introduced and impulse response of the n'th multipath component.

Similarly, for the secondary transmission, the interference signal received at the DTV broadcast receiver from the sec-

ondary transmitter $\text{UE}_{\text{sec}}^{(1)}$ is $r^{(S)}(t)$ would be:

$$r^{(S)}(t) = \frac{e^{j2\pi\Delta f^{(S)}t}}{\sqrt{T_u^{(S)}}}\left(\sum_{l\in\mathbb{Z}}\sum_{n=1}^{L}\sum_{k=0}^{N^{(S)}-1} h_n^{(S)} X_k^{(S)}[l] e^{j2\pi\frac{k'(t-\tau_n+t_{\text{off}})}{T_u^{(S)}}} \times \prod\left(\frac{t - lT^{(S)} + T_g^{(S)} - \tau_n + t_{\text{off}}}{T^{(S)}}\right)\right). \quad (3)$$

Here, L, τ_n, and $h_n^{(S)}$ are respectively the number of multipath components, delay introduced, and impulse response of the nth multipath component of secondary signal. $X_k^{(S)}$ is the data symbol transmitted in lth block on the kth subcarrier. $\Delta f^{(S)}$ is the frequency offset between the DTV and secondary signals. t_{off} is the delay offset introduced due to lack of synchronization of symbol start boundaries of the DTV and secondary OFDM symbols at the receiver. t_{off} is assumed to be a uniformly distributed random variable in $(0, T_u^{(D)})$. l indexes the secondary symbols received during the period $T_u^{(D)}$. Considering each secondary symbol duration as a time slot, let ξ' be the number of time slots a secondary signal is transmitted within one DTV broadcast symbol duration. With $T_u^{(D)} \gg T_u^{(S)}$, ξ' can take a value in $(0, \xi'_{\max})$, where $\xi'_{\max} = \left\lceil \frac{T_u^{(D)}}{T^{(S)}} \right\rceil$. Interference caused by the secondary signal at DTV receiver can vary depending on the number of active subcarriers $N^{(S)}$ and the number of occupied time slots ξ'. The DTV receiver processes both signals using the same basis functions. The OFDM decomposition basis function for m'th DVB symbol's p'th subcarrier is expressed as:

$$\Phi_{p',m'}^{(D)} = \frac{1}{\sqrt{T_u^{(D)}}} e^{-j2\pi\frac{p't}{T_u^{(D)}}} \prod\left(\frac{t - m'T^{(D)}}{T_u^{(D)}}\right). \quad (4)$$

For the DTV signal, the desired OFDM symbol at the p'th subcarrier in the m'th block is expressed as:

$$\tilde{X}_{p'}^{(D)}[m'] = X_{p'}^{(D)}[m'] H_{p'}^{(D)}[m'] \quad (5)$$

where $\tilde{X}_p'^{(D)}[m'] = \int_{\mathbb{R}} r^{(D)}(t)\Phi_{p',m'}^{(D)}(t)dt$ and $H_{p'}^{(D)} = \sum_{n'=1}^{(S)} h_{n',k'}^{(D)} e^{-j2\pi\frac{k'\tau_{n'}}{T_u^{(D)}}}$. For the interference signal $I_{p'}$ at the p'th subcarrier and m'th block,

$$I_{p'}[m'] = \int_{\mathbb{R}} r^{(S)}(t)\Phi_{p',m'}^{(D)}(t)dt. \quad (6)$$

Solving (6) for the general case yields (7), where $c(k) = \Delta f^{(S)} + \frac{k}{T_u^{(S)}} - \frac{p'}{T_u^{(D)}}$. The average interference power at the l'th subcarrier can then be expressed as:

$$\mathbb{E}[\mid I_{p'} \mid^2] = \frac{1}{T_u^{(S)} T_u^{(D)}} \sum_{k=0}^{N_L-1} \mid H_k^{(S)} \mid^2 \times \left\{ \sum_{b=0}^{\lfloor\xi'\rfloor-1} \frac{\sin^2(\pi c(k) T^{(S)})}{\pi^2 c^2(k)} + \frac{1}{\pi^2 c^2(k)} \frac{T_1 + T_2}{T^{(S)}} \right\}. \quad (8)$$

where T_1 and T_2 are obtained as:

$$T_1 = \frac{T^{(S)}}{2} - \frac{\sin(2\pi c(k)(\tau_n + T^{(S)} - T_g^{(S)}))}{4\pi c(k)} + \frac{\sin(2\pi c(k)(\tau_n - T_g^{(S)}))}{4\pi c(k)} \quad (9)$$

$$T_2 = \frac{T^{(S)}}{2} - \frac{\sin(2\pi c(k)((\xi' - \lfloor\xi'\rfloor)T^{(S)} + \tau_n - T_g^{(S)}))}{4\pi c(k)} + \frac{\sin(2\pi c(k)((\xi' - \lfloor\xi'\rfloor)T^{(S)} + \tau_n - T_g^{(S)} - T^{(S)}))}{4\pi c(k)}. \quad (10)$$

The complete proof is provided in Appendix A. With uniform power allocation across all subcarriers, the SINR γ_{dtv} at the DTV receiver Rx_{dtv} can be expressed in terms of the average received power due to the broadcast transmitter $P_{rx}^{(D)}$, average received power due to the secondary transmitter $P_{rx}^{(S)}$, and the noise power at the DTV receiver N_o, as [10], [26]:

$$\gamma_{dtv} = \frac{P_{rx}^{(D)} E\left[\mid H^{(D)} \mid^2\right]}{P_{rx}^{(S)} E\left[\mid I^{(S)} \mid^2\right] + N_o}. \quad (11)$$

Equation (11) yields the impact of secondary signal on DTV reception performance. Since the DTV receivers do not transmit back to the DTV transmitters, the received DTV signal power $P_{rx}^{(D)}$ and interference power $P_{rx}^{(S)}$ at any DTV receiver that might be located in a secondary transmitter's coverage area is not known to the secondary transmitter. Under such circumstances, the secondary transmitter must ensure that interference in its coverage area caused to a DTV receiver stays below a threshold. This problem of deciding the secondary system's operating parameters in absence of any DTV receiver information is analyzed in the following section.

V. Formulation on Interference Aware Secondary QoS: The LSIP Transmission Scheme

While deploying a secondary system in a DTV coverage region, it is imperative that the SINR margin for DTV reception is maintained. The SINR margin depends on various parameters. The MCS scheme and Fast Fourier Transform (FFT) size employed by the DTV broadcast decide the limit of interference that a DTV receiver can tolerate. A higher FFT size reduces interference margin. Also, a higher MCS implies that the system is more susceptible to interference. Once decided, these parameters do not change for a long time in a DTV deployment. Thus, the SINR threshold for a DTV network can be considered reasonably static [32].

Consider the DTV broadcast transmitter Tx_{dtv} having a typical transmit power of $P_{tx}^{(D)}$ and the secondary transmitter $\text{UE}_{\text{sec}}^{(1)}$ have a maximum transmit power of $P_{tx}^{(S)}$. Then, as shown in the Fig. 2, for a given secondary transmitter location and its transmit power, there is a minimum distance around it (considering omnidirectional secondary transmission) within which the C/I ratio of the DTV receiver is below a threshold for a given set of DTV transmit and receive parameters. That is, if there is an active DTV receiver within that vicinity of the secondary transmitter, the interference experienced at the

$$I_{p'}[m'] = \frac{1}{\sqrt{T_u^{(D)} T_u^{(S)}}} \Bigg[\sum_{k=0}^{N^{(S)}-1} H_k^{(S)} e^{j2\pi \frac{k t_{\text{off}}}{T_u^{(S)}}} \Bigg(X_k^{(S)}[l] \frac{\sin(\pi c(k)((lT^{(S)} + \tau_n - t_{\text{off}} - T_g^{(S)}))}{\pi c(k)} \times e^{j\pi c(k)(lT^{(S)} + \tau_n - t_{\text{off}} - T_g^{(S)})}$$
$$+ \sum_{b=1}^{\lfloor \xi' \rfloor - 1} X_k^{(S)}[l+b] \frac{\sin(\pi c(k) T^{(S)})}{\pi c(k)} \times e^{j\pi c(k)((2l+2b-1)T^{(S)} + 2\tau_n - 2t_{\text{off}} - 2T_g^{(S)})} \tag{7}$$
$$+ X_k[l + \lfloor \xi' \rfloor] \frac{\sin(\pi c(k)(\xi' T^{(S)} - (l + \lfloor \xi' \rfloor) T^{(S)} - \tau_n + t_{\text{off}} + T_g^{(S)}))}{\pi c(k)} \times e^{j\pi c(k)(\xi' T^{(S)} + (l + \lfloor \xi' \rfloor) T^{(S)} + \tau_n - t_{\text{off}} - T_g^{(S)})} \Bigg) \Bigg].$$

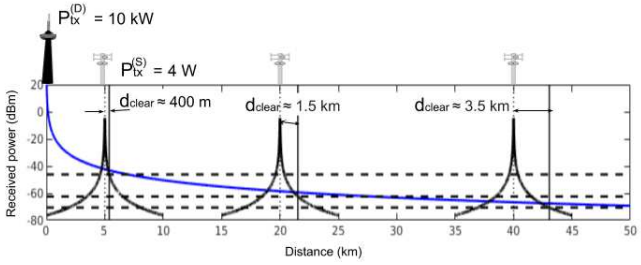

Fig. 2. Power and clearance distance margins at different secondary transmitter distances (d_A, cf. Fig. 1), with considered $P_{tx}^{(D)}$ = 10 W and $P_{tx}^{(S)}$ = 4 W.

DTV receiver is unacceptably high. In other words, if the DTV receiver distance from the secondary transmitter d_{st-dr} is larger than a minimum value, it is safe for the secondary transmitter to transmit without affecting the DTV reception performance. This minimum distance is defined as d_{clear}.

Naturally, d_{clear} depends on the received DTV power $P_{rx}^{(D)}$; $P_{rx}^{(D)}$ decreases as the distance from Tx_{dtv} increases. Conversely, for a known distance d_{st-dr} between $\text{UE}_{\text{sec}}^{(1)}$ and the nearest DTV receiver Rx_{dtv}, there is a maximum allowable transmit power $P_{tx}^{(S)}$ for the secondary node that keeps interference below the threshold. This maximum $P_{tx}^{(S)}$ decreases with increasing distance from Tx_{dtv}. Correspondingly, a secondary transmitter nearer to the Tx_{dtv} is expected to have a higher transmit margin of $P_{tx}^{(S)}$. For a fixed distance between secondary nodes and a given $P_{tx}^{(S)}$, a higher MCS may be employed to achieve higher data rates in locations closer to the DTV transmitter. Intuitively, as the distance from the DTV transmitter increases, the achievable secondary data rate drops.

Since no direct information on the distance between $\text{UE}_{\text{sec}}^{(1)}$ and the nearest DTV receiver Rx_{dtv} is available, the operational secondary transmission parameters must be conservative to reduce chance of interference level exceeding a predefined threshold at Rx_{dtv}. Computation of d_{clear} for the supported set of operating parameters can be done at $\text{UE}_{\text{sec}}^{(1)}$ using (11). Subsequently, an EPS algorithm is proposed that takes the value of d_{st-dr} into consideration to find the operational parameters that maximizes the secondary data rate.

In order to compute d_{clear}, the $\text{UE}_{\text{sec}}^{(1)}$ needs to find the relative positions of the secondary receiver $\text{UE}_{\text{sec}}^{(2)}$ and Tx_{dtv} with respect to itself. From the knowledge of received DTV signal strengths at the secondary transmitter and receiver and the received secondary signal strength at the secondary receiver, $\text{UE}_{\text{sec}}^{(1)}$ can calculate the position of $\text{UE}_{\text{sec}}^{(2)}$ on a 2-dimensional plane. Referring to Fig. 1 and considering the line joining the Tx_{dtv} and $\text{UE}_{\text{sec}}^{(1)}$ as the x-axis, the position of $\text{UE}_{\text{sec}}^{(2)}$ is $(d_B \cos\phi, d_B \sin\phi)$ where ϕ is computed from the sides of the triangle created between the peer nodes and the DTV transmitter as $\cos\ \phi = \dfrac{d_A^2 + d_B^2 - d_{AB}^2}{2 d_A d_B}$. Similarly, the angle θ between the secondary nodes with respect to the established x-axis is given as:

$$\cos\ (\pi - \theta) = \frac{d_A^2 + d_{AB}^2 - d_B^2}{2 d_A d_{AB}}. \tag{12}$$

Let the threshold SINR value of Rx_{dtv} for the given operating conditions be γ_{th}. $\text{UE}_{\text{sec}}^{(1)}$ must choose a set of operating parameters $(P_{tx}^{(S)}, R^{(S)}, N^{(S)}, \xi')$ which satisfy the constraints for successful secondary communication. Here, $P_{tx}^{(S)}$ is the secondary transmit power, $R^{(S)}$ is the MCS from the set $\mathbb{R}^{(S)}$, $N^{(S)}$ is the number of active subcarriers, and ξ' is the number of occupied time slots per DTV symbol.

For different sets of number of active subcarriers and number of time slots, expressed as $(N^{(S)}, \xi')$ pair, the effective value of secondary interference computed using (8) and (11) can be used to compute the received secondary power $P_{rx}^{(S)}$ at that distance. Clearly, for a lesser number of active subcarriers and less temporal occupancy, the $P_{rx}^{(S)}$ will be higher. Let this ratio be χ for the given set. For a fixed DTV transmit power $P_{tx}^{(D)}$ and some optimal secondary transmit parameter set chosen by the secondary transmitter $(P_{tx}^{(S)}, R^{(S)}, N^{(S)}, \xi')$, the ratio becomes larger than χ at a distance given by the positive solution of (13):

$$d_{\text{clear}} = d_A \left(\frac{\pm\sqrt{\cos^2\theta - (1 - \frac{1}{K})} - \cos\theta}{(1 - \frac{1}{K})} \right) \tag{13}$$

when same path-loss exponent is considered for both the networks. θ is obtained from (12), and $K = \left(\frac{\chi P_{d_0}^{(S)}}{P_{d_0}^{(D)}} \right)^{\frac{2}{\eta}}$. $P_{d_0}^{(D)}$ and $P_{d_0}^{(S)}$ are the powers received at the reference distances in the far-field region for Tx_{dtv} and $\text{UE}_{\text{sec}}^{(1)}$, respectively. When different path-loss exponents are considered, d_{clear} can be

expressed as:

$$d_{\text{clear}} = \left(\frac{P_{tx}^{(S)}}{P_{tx}^{(D)}} \chi d_a^{\eta^{(D)}} \right)^{\frac{1}{\eta^{(S)}}}. \quad (14)$$

The proof for (13) and (14) is provided in Appendix B.

Then, secondary communication is considered feasible if:

1) the distance after which DTV system's SINR γ_{dtv} stays strictly above γ_{th}, i.e., $\gamma_{dtv} \geq \gamma_{th}$ is less than the distance between secondary nodes, $d_{\text{clear}} \leq d_{AB}$;
2) no broadcast receiver exists within d_{clear} distance of the secondary transmitter in the direction of the receiver, $d_{\text{clear}} \leq d_{st-dr}$;
3) there exists a set $(P_{tx}^{(S)}, R^{(S)}, N^{(S)}, \xi')$ for the secondary transmitter which satisfies the minimum SNR constraint for the secondary reception at that MCS;
4) the minimum rate guarantee for the secondary system is fulfilled.

The secondary transmission fulfilling the above constraints by optimal parameter selection is termed as low interference secondary parameter selection based transmission, or LISP transmission scheme. When maximizing the secondary data rate for the given positions of Tx_{dtv}, $\text{UE}_{\text{sec}}^{(1)}$, and $\text{UE}_{\text{sec}}^{(2)}$ while keeping the SINR above a threshold value, the optimization problem for LISP transmission scheme can be stated as:

$$\underset{(P_{tx}^{(S)}, R^{(S)}, N^{(S)}, \xi')}{\text{maximize}} \quad rate(P_{tx}^{(S)}, R^{(S)}, N^{(S)}, \xi') \quad (15a)$$

$$\text{subject to} \quad \gamma_{dtv} \geq \gamma_{th} \quad (15b)$$

$$SNR^R \geq SNR^R_{\min} \quad (15c)$$

$$P_{tx}^{(S)} > 0 \quad (15d)$$

$$N^{(S)} > 0,\ N^{(S)} \in \{1, 2, \ldots, N^{(S)}_{\max}\} \quad (15e)$$

$$\xi' > 0,\ \xi' \in \{1, 2, \ldots, \xi'_{\max}\} \quad (15f)$$

$$R^{(S)} \in \mathbb{R}^{(S)}. \quad (15g)$$

The constraint of minimum SINR at the DTV receiver limits the secondary transmit power for the selected number of active subcarriers $N^{(S)}$, time slots ξ', and MCS $R^{(S)}$ through (15b). At the same time, the constraint of minimum SNR $SNR^R_{\min}$ for the chosen MCS $R^{(S)}$ in the secondary link suggests to have a higher $P_{tx}^{(S)}$ through (15c). The constraint of maintaining d_{clear} would change the distance value in the constraint (15b). A minimum data rate requirement can also be added as a constraint to the above formulation, though it is simpler to have a simple conditional check if the value of maximum data rate achieved through the above analysis satisfies the data rate. This maximization problem involves finding the optimal parameters in a finite subspace involving a combination of discrete and continuous variables.

This problem can be solved by first considering the continuous variable, i.e. transmit power $P_{tx}^{(S)}$. The required $P_{tx}^{(S)}$ for all combinations of the remaining parameters can be computed first. Since the number of MCS used is small and fixed, this creates the boundary values of usable power levels, leading to discretization of the power values. Then, all variables involved in the problem become discrete. Since this subset space of configurations is relatively small (of the order $| \mathbb{R}^{(S)} | \times N^{(S)}_{\max} \times \xi'_{\max}$ where $| \mathbb{R}^{(S)} |$ is the number of MCS schemes), an exhaustive search method is employed to find the optimal solution to the above problem. The proposed EPS algorithm to solve the problem is described in Algorithm 1.

When more than one physical transmission schemes are available, the EPS algorithm may be used on both to select the one which yields better data rate for the same constraint.

Since the power ratios are invariant of distances, for fixed physical layer schemes (WiFi and LTE), these values can be pre-computed and saved as tables for different combinations of subcarrier and time slots. With such pre-computation, the EPS algorithm has a worst case time complexity of $O(| \mathbb{R}^{(S)} | .N^{(S)}_{\max}.\xi'_{\max})$. Since the available range of MCS, the number of subcarriers, and the number of secondary time slots available per DTV symbol duration are small values, the EPS algorithm is easily executable at the secondary transmitters.

In the next section, co-channel interference analysis is validated via extensive experiments and simulations. Then, the performance of LISP transmission is studied and insights on feasibility/limits of such transmissions are drawn.

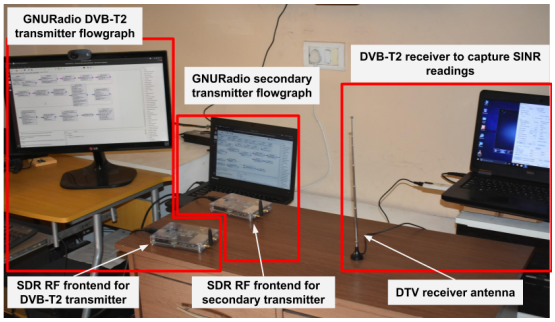

Fig. 3. Experimental setup to study the effects of co-channel secondary transmission on DTV reception.

VI. Experimental Studies and Results

First, the experimental method is explained:

A. Experimental methodology

1) DTV broadcast network: The experimental verification of interference analysis was first conducted in an outdoor rooftop environment using the regional DTV signal as the desired signal source, an inexpensive commercial off-the-shelf (COTS) DTV receiver for receiving the broadcast, and a Software Defined Radio based implementation of an interference source. Despite fluctuations due to environmental factors across various iterations, the rooftop reception of the DTV signal maintained an excellent SNR range for reception purposes. Thus, multipath fading effects were considered negligible in the presence of a strong DTV signal. However, this range of variation in the receied power levels at the DTV receiver made the measurements of secondary performance inaccurate. Consequently, rest of the experiment was performed in a controlled indoor setting to maintain steady SNR values as is detailed further. Since the effects of interference were

Algorithm 1: Maximization of secondary data rate: Exhaustive parameter search (EPS) algorithm

Result: Parameter set $(P_{tx}^{(S)}, R^{(S)}, N^{(S)}, \xi')$ that maximizes data rate
Initialize $d_{\mathtt{clear}}, d_A, d_B, d_{AB}$;
Initialize $P_{tx}^{(D)}$;
Initialize $\mathbb{R}^{(S)}$;
Initialize γ_{th} ;
Initialize $rate_{\min}$;
$rate_{\max} \leftarrow 0$;
$subcarriers \leftarrow 0$;
$slots \leftarrow 0$;
$modulation \leftarrow 0$;
$P_{tx}^{(S)} \leftarrow 0$;
for $N^{(S)} \leftarrow 1$ ***to*** $N_{\max}^{(S)}$ **do**
  for $\xi' \leftarrow 1$ ***to*** $\xi'_{\max}$ **do**
    $\chi(N^{(S)}, \xi') = \mathtt{power\_ratio}(\gamma_{th}, N^{(S)}, \xi')$;
    $P_{rx}^{(S)} \leftarrow$ $\mathtt{rx\_power}(\chi(N^{(S)}, \xi'), d_{\mathtt{clear}}, d_1, d_2, d_{AB}, P_{tx}^{(D)})$;
    $P_{tx_A}^{(S)}(\chi(N^{(S)}, \xi') \leftarrow \mathtt{tx\_power}(P_{rx}^{(S)}, d_{\mathtt{clear}})$;
  end
end
for $R^{(S)} \in \mathbb{R}^{(S)}$ **do**
  Initialize $SNR_{\min}^{R}$;
  $rate_{eff} = \mathtt{code\ rate} \times \mathtt{bits\ per\ symbol}$;
  for $N^{(S)} \leftarrow 1$ ***to*** $N_{\max}^{(S)}$ **do**
    for $\xi' \leftarrow 1$ ***to*** $\xi'_{\max}$ **do**
      $D(R^{(S)}, N^{(S)}, \xi') = \frac{N^{(S)}.\xi'.rate_{eff}}{T_s^{(D)}}$;
      $P_{rx}^{(S)} \leftarrow \mathtt{rx\_power\_from\_snr}(SNR_{\min}^{R})$;
      $P_{tx_B}^{(S)}(R^{(S)}, N^{(S)}, \xi') \leftarrow \mathtt{tx\_power}(P_{rx}^{(S)}, d_{AB})$;
      if $P_{tx_A}^{(S)} \geq P_{tx_B}^{(S)}$ ***and*** $D(R^{(S)}, N^{(S)}, \xi') > rate_{\max}$ **then**
        $rate_{\max} \leftarrow D(R^{(S)}, N^{(S)}, \xi')$;
        $subcarriers \leftarrow N^{(S)}$;
        $slots \leftarrow \xi'$;
        $modulation \leftarrow R^{(S)}$;
        $P_{tx}^{(S)} \leftarrow P_{tx_B}^{(S)}$;
      end
    end
  end
end
if $rate_{\max} \geq rate_{\min}$ **then**
  $\mathtt{return}(modulation, subcarriers, slots, P_{tx}^{(S)})$;
else
  $\mathtt{return}(0, 0, 0, 0)$;
end

TABLE II
DTV (DVB-T2) TRANSMISSION PARAMETERS

Center frequency	429 MHz
Bandwidth	7.6094 MHz (8 MHz)
FFT size	4096
Active subcarriers	3409
Guard interval fraction	1/32
Code rate	2/3
Modulation	64 QAM
Symbol duration	448 μs

TABLE III
SECONDARY TRANSMITTER PARAMETERS

	LTE-like	802.11af-like
Bandwidth	4.703 MHz (5 MHz)	6.33 MHz (8 MHz)
FFT size	512	128
Active subcarriers	301	108
Guard interval fraction	1/4	1/4
Modulation	QPSK	QPSK
Symbol duration	66.6 μs	22.5 μs
Maximum time slots	7	20

TABLE IV
RECEIVER SENSITIVITIES FOR SUPPORTED SECONDARY MCS (IN dBm)

Code rate \ Modulation scheme	QPSK	16-QAM	64-QAM
1/8	-5.1	-	-
1/4	-1.7	-	-
1/2	2.0	7.9	-
2/3	4.3	11.3	15.3
3/4	5.5	12.2	17.5
4/5	-	-	18.6

measured at the DTV receiver in the form of SINR, the distance between various nodes in the setup does not impact the observed behavior.

DVB-T2 is used with parameters listed in Table II. The transmitter chain is implemented in GNU-Radio. The COTS DTV receiver as shown in the Fig. 3 is used, to ensure that the observations are as close to a typical deployment scenario. Performance is studied with the DTV receiver having a good SNR in absence of any interference. It is observed that, with the considered DTV system parameters, a minimum SNR of 14 dB ensures a good reception quality.

2) Secondary network: The secondary transmitter supports two sets of transmission parameters, both implemented in GNU Radio: (a) an OFDM transmitter chain with LTE-like parameters and (b) an 802.11af like transmitter chain. The parameters used are listed in Table III. Note that, these transmission schemes do not use framing structures of the respective standards; only the physical layer parameters, such as the number of active subcarriers and bandwidth, are similar.

The parameters to be used for secondary transmission can be chosen from the two sets. Gated transmission is implemented where the duration of transmission is controllable. Transmit power and its center frequency can also be varied. Being an opportunistic network, it is assumed that the secondary system is fully capable of operating in presence of a strong DTV signal by knowing the DTV signal structure and employing appropriate interference cancellation techniques.

For simulations, the secondary signal stream consists of a baseband OFDM signal where the subcarriers overlapping with the broadcast signal are modulated according to the scheme mentioned in Table III. The time-domain signal is adjusted to account for the duration in a DVB-T2 signal's symbol period when the secondary does not transmit. The received time-domain secondary signal is re-sampled using `sinc` interpolation, and the excess samples generated are dropped to match the number of samples required for DTV signal reception. This signal is then processed using the DTV system parameters, and the average power over the DTV system subcarriers is calculated. For analyzing the QoS of the secondary system, the secondary transmitter uses a maximum

power level of 23 dBm and from MCS schemes typical of a LTE user equipment from Table IV. The entries in Table IV reflect the minimum SNR value for acceptable reception quality for the selected MCS.

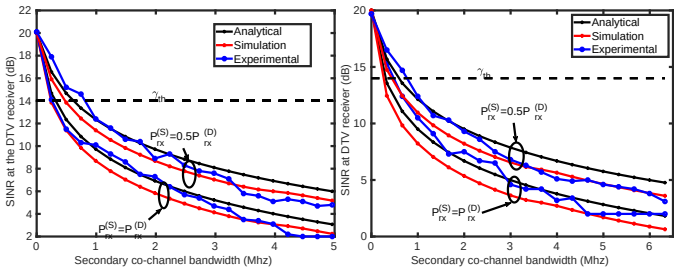

(a) (b)

Fig. 4. SINR at DTV receiver versus spectral overlap, with (a) LTE-like secondary transmission, symbol period $T_u^{(S)}$: 66.6 μs, subcarrier spacing: 15 kHz; (b) IEEE 802.11af-like secondary transmission, $T_u^{(S)}$: 22.5 μs, subcarrier spacing: 55.5 kHz.

3) Experimental procedure: The DTV transmitter and receiver were placed at a fixed distance. DTV transmit power was set such that the received SNR was 20 dB. A MPEG transport stream was used as the payload. The BER reported in the debugging interface of the COTS DTV receiver was insufficient in terms of precision to measure the reception quality in terms of Quasi Error Free (QEF) conditions [33], an equivalent measure defined by ITU-R as Subjective Failure Point (SFP) [34] was used where the reception to be correct if not more than one frame error is visible over an average period of 20 seconds.

A calibrated SDR was used as a secondary transmitter. Secondary receiver was co-located with the DTV receiver. Secondary transmit power was set such that the secondary's received SNR is 20 dB when exclusively receiving the secondary transmission. A random bit stream is used as the payload.

The secondary transmitter is initially set to transmit all the time slots in the adjacent channel. The amount of spectral overlap is increased by shifting its center frequency into the DVB-T2 channel in small increments (0.25 MHz for LTE-like system, and 0.3 MHz for 802.11af-like system). For each spectral overlap, SINR at the DTV receiver is measured.

Similarly, the overlapped time slots is varied from full occupancy (7 slots for LTE-like system, and 20 slots for 802.11af-like system) to no occupancy. The entire procedure is repeated at lower power levels for both secondary variants.

To study the effects of subcarrier density, bandwidth B is held constant at 5 MHz. The number of active subcarriers (M) is chosen iteratively from $[64, 128, 256, 512]$. Then, for complete spectral overlap, the performance of each setting was observed and compared with the analytical results.

The results that follow compare the analytically estimated performance with simulations and experimental observations.

B. DTV reception interference performance

1) Variable frequency overlap: DTV broadcast reception performance is studied here with varying spectral overlap, at two different received secondary power levels. The analytical and simulation results are compared with the experimental data in Figs. 4a and 4b for the two transmission schemes: LTE-like and 802.11af-like. The extent of degradation is comparable in both the schemes for a given spectral overlap. This is also supported by the results from analytical expressions in (8) and (11). For brevity, one-to-one comparative figure is omitted. It is also observed that, at a reduced secondary power at the DTV receiver an increased spectral over is tolerated.

2) Variable temporal occupancy: For a fixed secondary transmit power and full spectral overlap of secondary with the DTV band, Figs. 5a and 5b show DTV reception performance at different temporal occupancy. It is noted that, the degradation of SINR due to increased temporal occupancy is more severe than that with a similar fractional increase in spectral overlap. As it can be observed from (8), each slot adds to the overall interference at the DTV receiver. Consequently, DTV reception performance drops with every occupied time slot.

It is also apparent that 802.11af-like scheme offers a greater granularity for the amount of temporal occupancy as compared to LTE-like system. At the same time, there is a loss of granularity in the amount of spectral overlaps.

With SINR threshold 14 dB, neither pure spectral overlap nor pure temporal overlap yields feasible secondary networks operation. However, these two dimensions being orthogonal, a mixed mode that operates jointly in time and frequency dimensions is likely to give better performance.

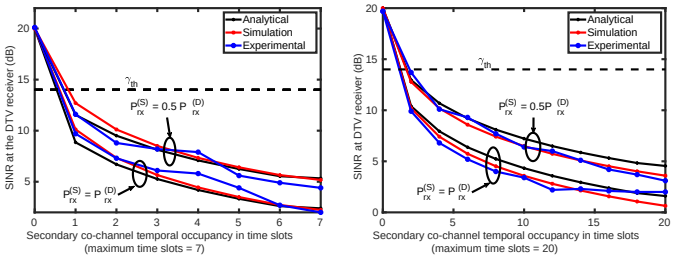

(a) (b)

Fig. 5. SINR DTV receiver versus time occupancy, with (a) LTE-like secondary transmission, symbol period $T_u^{(S)}$: 66.6 μs, subcarrier spacing: 15 kHz, maximum secondary time slots per DTV OFDM symbol: 7; (b) IEEE 802.11af-like secondary transmission, $T_u^{(S)}$: 22.5 μs, subcarrier spacing: 55.5 kHz, maximum secondary time slots per DTV OFDM symbol: 20.

3) Variable subcarrier density: So far, two schemes having different bandwidth and subcarrier densities among other parameters have been compared. Comparable performance with similar spectral overlaps are observed; also each occupied time slot adds to the overall interference. Then, it is likely that the different transmission schemes having the same spectral overlap and time occupancy would yield similar performance irrespective of their subcarrier densities. In Fig. 6, for a fixed spectral overlap of 5 MHz and secondary transmitter power set at $P_{rx}^{(S)} = 0.25P_{rx}^{(D)}$, DTV performance with varying secondary system's subcarrier density and number of time slots is observed. Time occupancy is expressed in terms of fraction of DVB-T2 symbol time. Indeed it is observed that, for the same time occupancy, various subcarrier densities incur comparable DTV performance. Thus, the secondary

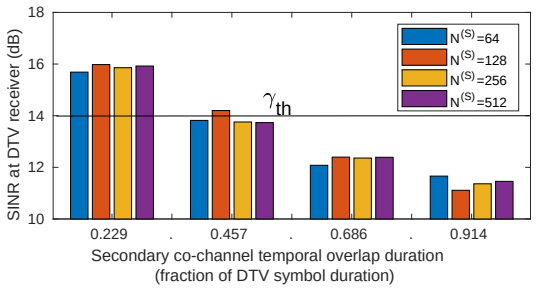

Fig. 6. SINR variation with different time occupancy fractions and subcarrier density ($P_{rx}^{(S)} = 0.25P_{rx}^{(D)}$).

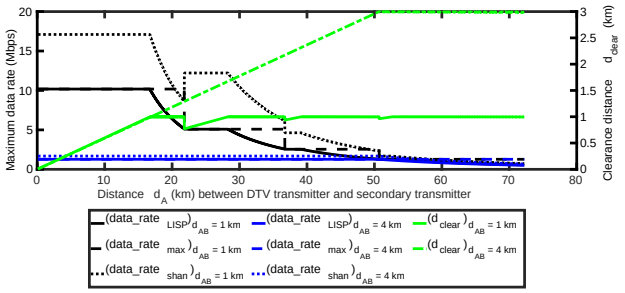

Fig. 7. Maximum achievable throughput over a secondary link with fixed separation between the secondary nodes.

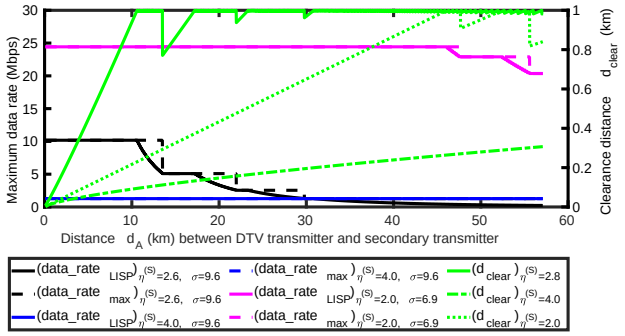

Fig. 8. Maximum achievable throughput over a secondary link with fixed separation between the secondary nodes for different propagation profiles d_{ab} = 1 km.

transmission performance can be controlled by the granularity in terms of spectral overlap and temporal occupancy.

It is observed that the SINR performance at a DTV receiver is more sensitive to variation in temporal occupancy as compared to variation in spectral overlap. Further, the performance is least affected by the choice of subcarrier density in the secondary transmission as long as temporal and spectral occupancy remain the same. This in turn, allows the use of spectral overlaps and temporal occupancy in a complementing way by allowing flexibility in choosing the number of subcarriers and symbol duration to sustain secondary transmissions while keeping the SINR at DTV receivers below a threshold.

C. Secondary QoS performance

The results so far have demonstrated the possibility of successful co-channel secondary transmission. Performance of the secondary system using the proposed LISP transmission scheme (in Section V) that selects the best parameters to maximize the data rate, is evaluated next. The following scenarios are studied: The maximal achievable data rate using the same power as employed by the proposed LISP scheme is considered as a benchmark. Further, Shannon data rate scaled by the coding rate being used by the two schemes is considered as an upper bound of performance for the parameters using in the LISP scheme. A suburban terrain is considered for the majority of path-loss computations. To this end, a macro-cell path loss exponent of 2.8 is considered for the DTV signal, while a micro-cell path loss of 2.6 is considered for the secondary signal. However, it is noted that small differences in the path-loss exponents do not affect the performance by a large amount and the same values may also be considered. The effects of log-normal shadowing are also assumed to be similar for both signals due to a shared environment with a standard deviation of 9.6 dB [35]. The power selection for the secondary transmitter maintains an outage constraint of 0.1.

1) Effect of distance between secondary transmitter and DTV transmitter: For a few representative secondary transmitter-receiver distances, secondary throughput versus distance between the DTV transmitter Tx_{dtv} and a secondary transmitter $\text{UE}_{\text{sec}}^{(1)}$ is shown in Fig. 7. $\text{UE}_{\text{sec}}^{(1)}$ uses LISP transmission scheme while working with transmission parameters listed in Table III and MCS levels listed in Table IV.

The main constraint on the parameter set selection is $d_{\text{clear}} \leq d_{st-dr}$. A throughput up to 10 Mbps is achievable within 18 km range from Tx_{dtv} when secondary transmitter-receiver distance is $d_{AB} = 1$ km. As the distance from Tx_{dtv}, d_A increases, power margin available for the secondary link decreases, which restricts the choice of usable MCS. The requirement of d_{clear} for the secondary link also increases. This is reflected in the decline of achievable data rates with increased d_A, for different values of d_{AB}. The benchmark scheme consists of a steep step-wise descent as the available power margin reduces at those points. This is as it does not take into account the requirement of maintaining the clearance distance d_{clear} and would, consequently be causing interference. However, the LISP scheme adapts according to the requirement and gradually changes the number of subcarriers and time slots to keep the impact of interference low. Both schemes maintain rates at least 4 Mbps below the scaled Shannon data rates.

Figure 8 shows the variation of throughput and clearance distance for various path-loss exponents and shadowing coefficients. For a rural line-of-sight propagation profile ($\eta = 2.0, \sigma = 6.9$ dB), throughput of up to 25 Mbps is obtained even at large distances from the DTV transmitter for a secondary node separation of 1 km. For a typical suburban environment ($\eta = 2.6, \sigma = 9.6$ dB), throughput declines quickly and settles at the minimum 1.5 Mbps mark. Intuitively, minimum throughput is maintained for dense urban areas ($\eta = 4.0, \sigma = 9.6$ dB). Due to space constraints, the remainder of analysis is conducted with the suburban propagation model.

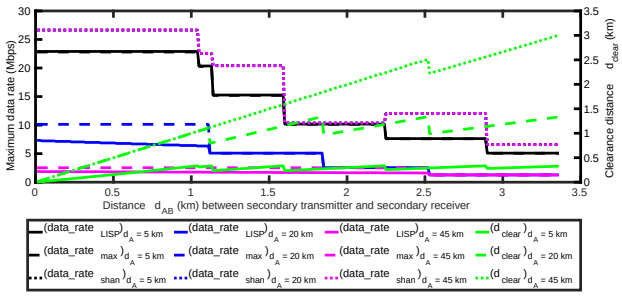

Fig. 9. Maximum achievable throughput in the secondary system link with fixed separation between the DTV transmitter and the secondary transmitter.

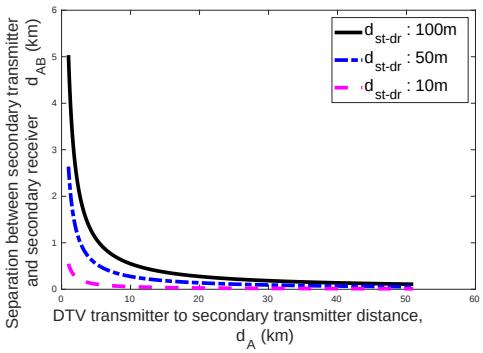

Fig. 10. Maximum secondary transmitter-receiver distance versus DTV transmitter to secondary transmitter distance subject to data_rate$_{\min}$ = 1Mbps.

2) Effect of distance between secondary nodes: To study the effect of secondary transmitter-receiver distance d_{AB} on link throughput, the distance d_A between Tx$_{\text{dtv}}$ and UE$_{\text{sec}}^{(1)}$ is fixed at three representative distances: near (5 km), moderately-far (20 km) and far (45 km). The results in Fig. 9 show that, at $d_A = 5$ km sharp drops in throughput occur at various inter-node separations. These drops become more gradual as d_{AB} increases. Note that the distances where such drops are observed align with the distances where d_{clear} also drops before starting to rise again. The drop in d_{clear} indicates a reduction of transmit power at UE$_{\text{sec}}^{(1)}$. Meanwhile, the benchmark cases retain their flat step-wise transitions, always maintaining a throughput higher than the proposed LISP scheme while also incurring interference at the DTV receivers.

At a high power setting, UE$_{\text{sec}}^{(1)}$ uses a lower number of subcarriers $N^{(S)}$ and a smaller number of time slots ξ' with a higher MCS $R^{(S)}$ to maximize the throughput. When the distance increases beyond a limit, the EPS algorithm reduces the transmit power and accordingly uses a lower MCS while increasing the values of $N^{(S)}$ and ξ' to compensate for the loss of data rate while meeting the SINR constraints. After each drop, d_{clear} continues to rise before the next drop while the throughput stays almost constant or decreases slowly. Thus, the EPS algorithm adjusts the secondary transmission parameters to compensate for the average interference that could be caused at a DTV receiver in the vicinity of the secondary link's coverage area.

Since the remaining two subsections deal with constraints on data rate and clearance distance d_{clear}, the benchmark case cannot be applied.

3) Effect of minimum data rate and separation constraints: So far, no external constraint on UE$_{\text{sec}}^{(1)}$ has been imposed. Now, with d_{st-dr} as the minimum distance between UE$_{\text{sec}}^{(1)}$ and Rx$_{\text{dtv}}$ and data_rate$_{\min}$ = 1Mbps, the maximum feasible distance between secondary nodes d_{AB} as a function of distance d_A between UE$_{\text{sec}}^{(1)}$ and Tx$_{\text{dtv}}$ is studied, as shown in Fig. 10. The three values of d_{st-dr} are considered to represent closely spaced (10 m), moderately spaced (50 m) to sparse density (100 m) broadcast receivers typical of rural populations. It is observed that d_{AB} quickly tapers off to less than a kilometer beyond 10 km from the DTV transmitter and gets smaller when d_A increases. While the trend stays

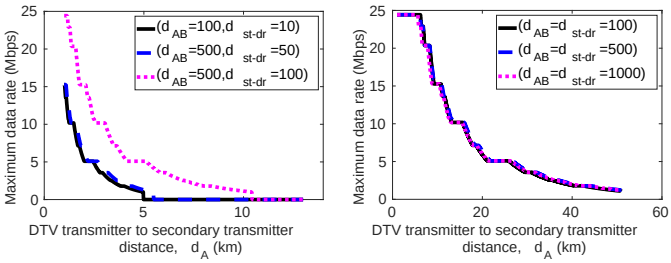

Fig. 11. Maximum achievable data rate at varying separation between the DTV transmitter and the secondary transmitter for data_rate$_{\min}$ = 1 Mbps with (a) unequal d_{st-dr} and d_{clear} (b) $d_{st-dr} = d_{\text{clear}}$.

the same, the separation distance is a function of link-budget parameters such as shadowing margin and fading margin. This is due to the availability of a minimal power margin at the secondary transmitter. This is further constrained when d_{st-dr} is small. Imposing high data rate requirements under these circumstances would make such a deployment infeasible.

4) Variation of coverage area of secondary network under minimum rate and separation constraints: Intuitively, certain system constraints may significantly restrict the scope of co-channel operation. The conditions where a co-channel secondary link may serve a larger area while providing reasonable data rate guarantees are explored in this subsection. To this end, the minimum rate requirement data_rate$_{\min}$, d_{AB}, and d_{st-dr} are held fixed. Fig. 11a shows the variation of throughput versus distance between Tx$_{\text{dtv}}$ and UE$_{\text{sec}}^{(1)}$. For the same secondary transmitter-receiver distance, the maximum distance between UE$_{\text{sec}}^{(1)}$ from Tx$_{\text{dtv}}$ which can support data_rate$_{\min}$ depends on the separation between DTV receivers d_{st-dr}. That is, to increase the coverage region of secondary networks around the DTV transmitter, d_{st-dr} must increase. This is observed in Fig. 11a, where the co-channel deployment allowing data_rate$_{\min}$ = 1 Mbps doubles from 5 km to 10 km for $d_{AB} = 500$ m when d_{st-dr} increases from 50 m to 100 m.

As a special case, the scenario where all DTV receivers are also secondary transmission capable, that is with $d_{st-dr} = d_{\text{clear}}$, is considered. The results in Fig. 11b show that, a secondary network providing up to 10 Mbps rate is feasible in an extensive area of 50 km around the DTV transmitter without exceeding DTV receivers' SINR threshold. Thus,

if the restriction of silent broadcast receivers is eliminated, considerable gains in throughput and coverage are achieved from such co-channel deployments. Further, the throughput profile is seen to be similar for all inter-secondary distances. This would be particularly useful in providing connectivity over sparsely populated regions.

VII. Concluding Remarks

In this work, a closed-form expression has been developed for co-channel interference among heterogeneous OFDM systems involving DTV broadcast and secondary transmission with LTE-A or WiFi (802.11af) based technology. It has been observed that, different secondary communication schemes having comparable parameters, like spectral and temporal overlaps, on DTV reception have similar impact. Thus, the choice of secondary OFDM transmission strongly depends on its data rate requirements as well as the system parameters.

Subsequently, the expression for interference has been used to develop the low interference secondary parameter selection based transmission scheme (LISP) for selecting best parameters for an OFDM-based co-channel secondary transmission in the DTV broadcast network area, subject to the condition that DTV reception SINR quality does not go below an acceptable threshold value. Specifically, the exhaustive parameter search (EPS) algorithm finds the operating parameters given various measurement data. The evaluation of secondary system performance suggests that, when the secondary transmitter-receiver distances are small and data rate requirements are also low, such a co-channel secondary network may be deployed across a large geographical region. This is particularly useful for low data rate applications like IoT communication networks. Such co-channel secondary deployment over TV spectrum can enable a variety of use cases ranging from low power in-building media distribution to machine-to-machine communications.

The efficacy of the proposed LISP scheme and EPS algorithm is contingent on the availability of information about the active DTV receivers' location and experienced SINR. Since all DTV receivers are hidden in the DTV broadcast network, this poses unique implementation challenges for the proposed scheme. Various aspects, ranging from detection of DTV receivers to obtaining their SINR values need to be explored in order to solve this challenge and ultimately creating a viable and intelligent secondary network that coexists with a DTV network in co-channel mode.

Appendix A
Co-channel Interference at DTV Receiver

The basis function (4) decomposes the received DTV signal (2) as well as the secondary signal (3) over the p'th DTV subcarrier and m'th OFDM symbol block of the DTV transmission. The secondary signal is unwanted at the DTV receiver as causes interference in reception. The interfering signal after decomposition using (4) can be expressed as:

$$\begin{aligned} I_{p'}[m'] =& \int_{\mathbb{R}} r^{(S)}(t)\Phi^{(D)}_{p',m'}(t)dt \\ =& \frac{1}{\sqrt{T_u^{(D)}T_u^{(S)}}}\left(\int_{\mathbb{R}}\sum_{l\in\mathbb{Z}}\sum_{n=1}^{L}h_n^{(S)}\sum_{k=0}^{N^{(S)}-1}X_k^{(S)}[l]\right. \\ & e^{j2\pi c(k)t}e^{-j2\pi\frac{k\tau_n}{T_u^{(S)}}}e^{-j2\pi\frac{kt_{\text{off}}}{T_u^{(S)}}}\prod\left(\frac{t-m'T^{(D)}}{T_u^{(D)}}\right) \\ & \left.\prod\left(\frac{t-lT^{(S)}-\tau_n+T_g^{(S)}+t_{\text{off}}}{T^{(S)}}\right)dt\right) \end{aligned} \tag{A.1}$$

where $c(k)=\Delta f^{(S)}+\frac{k}{T_u^{(S)}}-\frac{p'}{T_u^{(D)}}$. Clearly, the effective integration period in (A.1) depends on $\prod\left(\frac{t-m'T^{(D)}}{T_u^{(D)}}\right)$ and $\prod(\frac{t-lT^{(S)}-\tau_n+T_g^{(S)}+t_{\text{off}}}{T^{(S)}})$, which are the normalized windowing functions respectively for the DTV receiver's basis function and the secondary signal, expressed as:

$$\prod\left(\frac{t-m'T^{(D)}}{T_u^{(D)}}\right)=1 \text{ iff } m'T^{(D)}\le t\le T_u^{(D)}+m'T^{(D)} \tag{A.2}$$

$$\begin{aligned} \prod\left(\frac{t-lT^{(S)}-\tau_n+T_g^{(S)}+t_{\text{off}}}{T^{(S)}}\right)=1 \\ \text{iff } lT^{(S)}+T_r\le t\le(l+1)T^{(S)}+T_r \end{aligned} \tag{A.3}$$

where $T_r=\tau_n-t_{\text{off}}-T_g^{(S)}$. If ξ' secondary symbols are received in a DTV symbol's useful duration $T_u^{(D)}$, (A.1) can be expressed as the sum of interference due to each secondary signal. m' being the index of the DTV symbol under consideration, the value of m' does not affect the analysis. Hence, without loss of generality m' is taken as 0 in the subsequent analysis. Accordingly, ((A.1)) can be rewritten as:

$$\begin{aligned} I_{p'} =& \frac{1}{\sqrt{T_u^{(D)}T_u^{(S)}}}\left[\sum_{k=0}^{N^{(S)}-1}H_k^{(S)}e^{j2\pi\frac{kt_{\text{off}}}{T_u^{(S)}}}\right. \\ & \times\left\{\int_0^{lT^{(S)}+\tau_n-t_{\text{off}}-T_g^{(S)}}X_k[l].e^{j2\pi c(k)t}dt\right. \\ & +\sum_{b=1}^{\lfloor\xi'\rfloor-1}\int_{(l+b-1)T^{(S)}+\tau_n-t_{\text{off}}-T_g^{(S)}}^{(l+b)T^{(S)}+\tau_n-t_{\text{off}}-T_g^{(S)}}X_k[l+b]e^{j2\pi c(k)t}dt \\ & \left.\left.+\int_{(l+\lfloor\xi'\rfloor)T^{(S)}+\tau_n-t_{\text{off}}-T_g^{(S)}}^{\xi'T^{(S)}}X_k[l+\lfloor\xi'\rfloor]e^{j2\pi c(k)t}dt\right\}\right]. \end{aligned} \tag{A.4}$$

Solving (A.4) yields (7) for the general case. When $c(k)=0$, $I_{p'}$ can be expressed as:

$$\mathbb{E}\left[\mid I_{p'}^{(S)}[m]\mid^2\right]_{t_{\text{off}}} = \frac{1}{T_u^{(D)}T_u^{(S)}}\left|\sum_{k=0}^{N^{(S)}-1} H_k^{(S)} e^{j2\pi\frac{kt_{\text{off}}}{T_u^{(S)}}}\left[X_k^{(S)}[l]\frac{\sin\pi c(k)(T^{(S)}+\omega)}{\pi c(k)}e^{j\pi c(k)(T^{(S)}+\omega)}\right.\right. \tag{A.6}$$
$$\left.\left. + \sum_{b=0}^{\lfloor\xi'\rfloor-1} X_k^{(S)}[l+b]\frac{\sin\pi c(k)T^{(S)}}{\pi c(k)}e^{j\pi c(k)[(l+b-0.5)T^{(S)}+\omega]} + X[\lfloor\xi'\rfloor]\frac{\sin\pi c(k)[(\xi'-\lfloor\xi'\rfloor)T^{(S)}]}{\pi c(k)}e^{j\pi c(k)[(\xi'+\lfloor\xi'\rfloor)T^{(S)}+\omega]}\right]\right|^2.$$

$$\mathbb{E}\left[\mid I_{p'}^{(S)}[m]\mid^2\right]_{t_{\text{off}}} = \frac{1}{T_u^{(S)}T_u^{(D)}}\sum_{k=0}^{N^{(S)}-1}\mid H_k^{(S)}\mid^2\left\{\frac{\sin^2(\pi c(k)(T^{(S)}+\omega))}{\pi^2c^2(k)} + \sum_{b=0}^{\lfloor\xi'\rfloor-1}\frac{\sin^2(\pi c(k)T^{(S)})}{\pi^2c^2(k)} + \frac{\sin^2(\pi c(k)((\xi'-\lfloor\xi'\rfloor)T^{(S)}-\omega))}{\pi^2c^2(k)}\right\}. \tag{A.7}$$

$$I_{p'} = \frac{1}{\sqrt{T_u^{(D)}T_u^{(S)}}}\left[\sum_{k=0}^{N^{(S)}-1} H_k^{(S)} e^{j2\pi\frac{kt_{\text{off}}}{T_u^{(S)}}}\right. \tag{A.5}$$
$$\times\left\{X_k[l].(lT^{(S)}+\tau_n-t_{\text{off}}-T_g^{(S)}) + \sum_{b=1}^{\lfloor\xi'\rfloor} X_k[l+b]T^{(S)}\right.$$
$$\left.\left. + X_k[l+\lfloor\xi'\rfloor]((\xi'-l-\lfloor\xi'\rfloor)T^{(S)}-\tau_n+t_{\text{off}}+T_g^{(S)})\right\}\right].$$

The average interference power at the p'th subcarrier for a given t_{off} can be expressed as (A.6), where $\omega \triangleq \tau_n - t_{\text{off}} - T_g^{(S)}$. Interference caused by the subcarriers of the secondary signal on each of the DTV subcarriers is independent. Also, interference caused by each secondary symbol is independent. Therefore, (A.6) can be expressed as (A.7).

Substituting ω into (A.7) and averaging over t_{off}, we have:

$$\mathbb{E}\left[\mid I_{p'}^{(S)}[m]\mid^2\right] = \int_0^{T^{(S)}}\mathbb{E}[\mid I_{p'}^{(S)}[m]\mid^2]_{t_{\text{off}}}dt_{\text{off}}. \tag{A.8}$$

Solving (A.8) yields the result in (8). For $c(k) = 0$, $\mathbb{E}\left[\mid I_{p'}^{(S)}[m]\mid^2\right]$ can be expressed as:

$$\mathbb{E}\left[\mid I_{p'}^{(S)}[m]\mid^2\right] = \frac{\mid H_k^{(S)}\mid^2}{T_u^{(S)}T_u^{(D)}}\left\{\lfloor\xi'\rfloor{T^{(S)}}^2 + T_1 + T_2\right\}$$

APPENDIX B
EXPRESSION FOR CLEARANCE DISTANCE d_{CLEAR}

For a given threshold value of SINR γ_{th}, let the ratio of received DTV signal power to secondary power be χ. The coordinates of a DTV receiver at a distance d_{clear} from secondary node $\text{UE}_{\text{sec}}^{(1)}$ along d_{AB} is $(d_A + d_{\text{clear}}\cos\theta, d_{\text{clear}}\sin\theta)$. From the simplified path-loss model, the following expression holds:

$$\chi = \frac{\frac{P_{tx}^{(D)}}{{f^{(D)}}^2}\left(\frac{d_o}{(\sqrt{(d_A+d_{\text{clear}}\cos\theta)^2+(d_{\text{clear}}\sin\theta)^2})}\right)^{\eta^{(D)}}}{\frac{P_{tx}^{(S)}}{{f^{(S)}}^2}\left(\frac{d_o}{d_{\text{clear}}}\right)^{\eta^{(S)}}} \tag{B.1}$$

where $\eta^{(D)}$ and $\eta^{(S)}$ are respectively the path loss exponent of the DTV network and the secondary network. Similarly, $f^{(D)}$ and $f^{(S)}$ are the center frequencies for the DTV signal and the secondary signal respectively. For co-channel operation, $\left(\frac{f^{(S)}}{f^{(D)}}\right)^2$ stays close to 1. Then, (B.1) can be expressed as:

$$\chi = \frac{P_{tx}^{(D)}}{P_{tx}^{(S)}}\left(\frac{d_{\text{clear}}^{\eta^{(S)}}}{(\sqrt{(d_A+d_{\text{clear}}\cos\theta)^2+(d_{\text{clear}}\sin\theta)^2})^{\eta^{(D)}}}\right). \tag{B.2}$$

Since the operating conditions for both DTV and secondary network are similar, $\eta^{(S)}$ and $\eta^{(D)}$ are usually comparable. For such conditions, it has been observed that the impact of taking the two values as identical greatly simplifies the analysis without impacting the resulting solution. Under such assumption, solving (B.2) for d_{clear} yields (13). Further, when $\eta^{(S)}$ and $\eta^{(D)}$ differ by a large proportion, the observation that $d_A \gg d_{clear}$ can be used to simplify the expression for d_{clear} as given in (14).

REFERENCES

[1] A. Thakur, S. De, and G. Muntean, "Interference-aware co-channel transmission over DTV bands via partial frequency and time overlaps," in *Proc. IEEE ICC*, Shanghai, China, May 2019, pp. 1–6.

[2] S. Agarwal and S. De, "eDSA: Energy-efficient dynamic spectrum access protocols for cognitive radio networks," *IEEE Trans. Mob. Comput.*, vol. 15, no. 12, pp. 3057–3071, Dec. 2016.

[3] "Evolved Universal Terrestrial Radio Access (E-UTRA); Study on minimization of drive-tests in next generation networks," 3rd Generation Partnership Project (3GPP), Tech. Rep. 36.805, 01 2010, ver. 9.0.0.

[4] S. Agarwal and S. De, "Cognitive multihoming system for energy and cost aware video transmission," *IEEE Trans. Cognitive Commun. Netw.*, vol. 2, no. 3, pp. 316–329, Sep. 2016.

[5] A. J. Coulson, "Bit error rate performance of OFDM in narrowband interference with excision filtering," *IEEE Trans. Wireless Commun.*, vol. 5, no. 9, pp. 2484–2492, Sep. 2006.

[6] H. Wang, X. Zhang, and S. Wang, "Narrowband interference suppression in OFDM systems," in *Proc. Intl. Conf. Wireless Commun. Sig. Process.*, Yangzhou, China, Oct. 2016, pp. 1–6.

[7] T. Weiss, J. Hillenbrand, A. Krohn, and F. K. Jondral, "Mutual interference in OFDM-based spectrum pooling systems," in *Proc. IEEE VTC-Spring*, Milan, Italy, May 2004, pp. 1873–1877.

[8] Q. Bodinier, F. Bader, and J. Palicot, "Coexistence in 5G: Analysis of cross-interference between OFDM/OQAM and legacy users," in *Proc. IEEE Globecom Wksp.*, Washington, DC, USA, Dec. 2016, pp. 1–6.

[9] P. Dharmawansa, N. Rajatheva, and H. Minn, "An exact error probability analysis of OFDM systems with frequency offset," *IEEE Trans. Commun.*, vol. 57, no. 1, pp. 26–31, Jan. 2009.

[10] J. Lee, H. l. Lou, D. Toumpakaris, and J. M. Cioffi, "SNR analysis of OFDM systems in the presence of carrier frequency offset for fading channels," *IEEE Trans. Wireless Commun.*, vol. 5, no. 12, pp. 3360–3364, Dec. 2006.

[11] K. A. Hamdi, "Exact SINR analysis of wireless OFDM in the presence of carrier frequency offset," *IEEE Trans. Wireless Commun.*, vol. 9, no. 3, pp. 975–979, Mar. 2010.

[12] Y. Medjahdi, M. Terré, D. L. Ruyet, and D. Roviras, "Interference tables: A useful model for interference analysis in asynchronous multicarrier transmission," *EURASIP J. Adv. Sig. Process.*, vol. 2014, no. 1, p. 54, Apr. 2014.

[13] G. P. Villardi, H. Harada, F. Kojima, and H. Yano, "Multilevel protection to broadcaster contour and its impact on TV white space availability," *IEEE Trans. Veh. Technol.*, vol. 66, no. 2, pp. 1393–1407, Feb. 2017.

[14] A. Kumar, A. Karandikar, G. Naik, M. Khaturia, S. Saha, M. Arora, and J. Singh, "Toward enabling broadband for a billion plus population with TV white spaces," *IEEE Commun. Mag.*, vol. 54, no. 7, pp. 28–34, Jul. 2016.

[15] S. Roberts, P. Garnett, and R. Chandra, "Connecting Africa using the TV white spaces: from research to real world deployments," in *Proc. IEEE LANMAN*, Apr. 2015, pp. 1–6.

[16] N. C. Prasad, S. Deb, and A. Karandikar, "Feasibility study of LTE middle-mile networks in TV white spaces for rural India," in *Proc. IEEE PIMRC*, Sep. 2016, pp. 1–6.

[17] F. J. Martin-Vega, B. Soret, M. C. Aguayo-Torres, I. Z. Kovacs, and G. Gomez, "Geolocation-based access for vehicular communications: Analysis and optimization via stochastic geometry," *IEEE Trans. Veh. Technol.*, vol. 67, no. 4, pp. 3069–3084, Apr. 2018.

[18] M. Khaturia, S. Suman, A. Karandikar, and P. Chaporkar, "Spectrum sharing for LTE-A network in TV white space," in *Proc. Nat. Conf. Commun.*, Feb. 2018, pp. 1–6.

[19] S. Agarwal and S. De, "Rural broadband access via clustered collaborative communication," *IEEE/ACM Trans. Netw.*, vol. 26, no. 5, pp. 2160–2173, Oct. 2018.

[20] J. Ribadeneira-Ramírez, G. Martínez, D. Gómez-Barquero, and N. Cardona, "Interference analysis between digital terrestrial television (DTT) and 4G LTE mobile networks in the digital dividend bands," *IEEE Trans. Broadcast.*, vol. 62, no. 1, pp. 24–34, Mar. 2016.

[21] V. Popescu, M. Fadda, M. Murroni, and D. Giusto, "Coexistence issues for IEEE 802.22 WRAN and DVB-T2 networks," in *Proc. IEEE BMSB*, Nara, Japan, Jun. 2016, pp. 1–4.

[22] V. Popescu, M. Fadda, M. Murroni, J. Morgade, and P. Angueira, "Co-channel and adjacent channel interference and protection issues for DVB-T2 and IEEE 802.22 WRAN operation," *IEEE Trans. Broadcast.*, vol. 60, no. 4, pp. 693–700, Dec. 2014.

[23] V. Popescu, M. Fadda, and M. Murroni, "Performance analysis of IEEE 802.22 wireless regional area network in the presence of digital video broadcasting - second generation terrestrial broadcasting services," *IET Commun.*, vol. 10, no. 8, pp. 922–928, 2016.

[24] G. Martínez-Pinzón, N. Cardona, C. Garcia-Pardo, A. Fornés-Leal, and J. A. Ribadeneira-Ramírez, "Spectrum sharing for LTE-A and DTT: Field trials of an indoor LTE-A femtocell in DVB-T2 service area," *IEEE Trans. Broadcast.*, vol. 62, no. 3, pp. 552–561, Sep. 2016.

[25] L. Polak, O. Kaller, L. Klozar, and J. Prokopec, "Exploring and measuring the co-existence between LTE and DVB-T2-Lite services," in *Proc. TSP*, Rome, Italy, Jul. 2013, pp. 316–320.

[26] H. Bawab, P. Mary, J. F. Hélard, Y. Nasser, and O. Bazzi, "Spectral overlap optimization for DVB-T2 and LTE coexistence," *IEEE Trans. Broadcast.*, vol. 64, no. 1, pp. 70–84, Mar. 2018.

[27] M. El Tanab and W. Hamouda, "Resource allocation for underlay cognitive radio networks: A survey," *IEEE Commun. Surveys Tuts.*, vol. 19, no. 2, pp. 1249–1276, Second Quarter, 2017.

[28] B. Wild and K. Ramchandran, "Detecting primary receivers for cognitive radio applications," in *IEEE Symp. on New Frontiers in Dynamic Spectrum Access Networks (DySPAN)*, Nov 2005, pp. 124–130.

[29] X. Zhang and E. W. Knightly, "Watch: Wifi in active tv channels," *IEEE Trans. Cogn. Commun. Netw.*, vol. 2, no. 4, pp. 330–342, 2016.

[30] J. G. Webster, *The International Encyclopedia of Communication*. Oxford: Wiley-Blackwell Publishing, 2008, vol. 7.

[31] E. Dall'Anese, S. Kim, G. B. Giannakis, and S. Pupolin, "Power control for cognitive radio networks under channel uncertainty," *IEEE Trans. Wireless Commun.*, vol. 10, no. 10, pp. 3541–3551, Oct. 2011.

[32] I. Eizmendi, G. Prieto, G. Berjon-Eriz, I. Landa, and M. Velez, "Empirical DVB-T2 thresholds for fixed reception," *IEEE Trans. Broadcast.*, vol. 59, no. 2, pp. 306–316, Jun. 2013.

[33] "Digital Video Broadcasting (DVB): Implementation Guidelines for a Second Generation Digital Terrestrial Television Broadcasting System (DVB-T2)," European Telecommunications Standards Institute(ETSI), Tech. Rep. ETSI TS 102 991, 01 2010, v1.3.1.

[34] "ITU, Planning Criteria, Including Protection Ratios, for Digital Terrestrial Television Services in the VHF/UHF Bands," International Telecommunication Union (ITU), Tech. Rep. BT.1368-9, 12 2011, iTU Rec. ITU-R.

[35] T. Schwengler, "Wireless and Cellular Communications Class Notes for tlen-5510," Lecture Notes, 2019.

Anshul Thakur (S'19) received his B.Tech. degree in electronics and communication engineering from National Institute of Technology, Hamirpur, India, in 2011. He is currently working as a Senior Research Engineer with Center for Development of Telematics, Delhi, India, and pursuing his Ph.D. degree with Department of Electrical Engineering, Indian Institute of Technology Delhi, India. His research interests are broadly in communication networks, with emphasis on broadband wireless access, and next-generation networks.

Swades De (S'02-M'04-SM'14) is a Professor in the Department of Electrical Engineering at IIT Delhi. Before moving to IIT Delhi in 2007, he was a Tenure-Track Assistant Professor of Electrical and Computer Engineering at the New Jersey Institute of Technology (2004-2007). He worked as an ERCIM post-doctoral researcher at ISTI-CNR, Pisa, Italy (2004), and has nearly five years of industry experience in India on telecom hardware and software development (1993-1997, 1999). His research interests are broadly in communication networks, with emphasis on performance modeling and analysis. Current directions include energy harvesting sensor networks, broadband wireless access and routing, cognitive/white-space access networks, smart grid networks, and IoT communications. Dr. De currently serves as an Area Editor for the IEEE COMMUNICATIONS LETTERS and Elsevier Computer Communications, and an Associate Editor for the IEEE TRANSACTIONS ON VEHICULAR TECHNOLOGY, the IEEE WIRELESS COMMUNICATIONS LETTERS, and the IEEE NETWORKING LETTERS.

Gabriel-Miro Muntean (M'04, SM'17) is an Associate Professor with the School of Electronic Engineering, Dublin City University (DCU), Ireland, and Co-Director of the DCU Performance Engineering Laboratory. He has published over 400 papers in top-level international journals and conferences, authored four books and 21 book chapters, and edited six additional books. His research interests include quality, performance, and energy saving issues related to multimedia and multiple sensorial media delivery, technology-enhanced learning, and other data communications over heterogeneous networks. Dr. Muntean is an Associate Editor of the IEEE Transactions on Broadcasting, the Multimedia Communications Area Editor of the IEEE Communications Surveys and Tutorials, and chair and reviewer for important international journals, conferences, and funding agencies. Dr. Muntean is senior member of IEEE and IEEE Broadcast Technology Society.